Extended Abstracts of the 2020 International Conference on Solid State Devices and Materials, VIRTUAL conference, 2020, pp623-624

Superconducting Poly-SOI Layers by Boron Ion Implantation and UV Nanosecond Laser Annealing

R. Daubriac[1], P. Acosta Alba[1], S. Lequien[2], C. Marcenat[2], T. D. Vethaak[2], F. Nemouchi[1], F. Lefloch[2] and S. Kerdilès[1]

[1] Université Grenoble Alpes, CEA LETI, 17 Rue des Martyrs, 38000, Grenoble, France
[2] Université Grenoble Alpes, CEA IRIG, 17 Rue des Martyrs, 38000, Grenoble, France

Abstract

We report on the superconducting properties of heavily boron-doped poly-Silicon-On-Insulator (SOI) layers (33 nm thick) fabricated by ion implantation (B, 2.5 x 10^{16} cm^{-2}, 3 keV) and UV nanosecond laser annealing (UV-NLA, λ=308 nm, pulse duration=160 ns, 4 Hz repetition rate) under N_2 flow at atmospheric pressure, also called Pulsed Laser Induced Epitaxy (PLIE). We identified SOI full-melt as an operating point to obtain superconductivity. The average critical temperature of our layers was around 170 mK. Also, thanks to low temperature measurements coupled with magnetic field variations, we highlighted a type II superconductor behavior with a coherence length of hole pairs around 75 nm.

1. Introduction

Quantum computing is one of the most challenging fields of the 21st century from scientific and economical points of view. In solid state physics, two types of qubits have been proposed: spin/charge qubits and superconducting qubits [1-4]. Silicon is one of the well-known materials for integration that also shows superconducting properties. For this reason, it constitutes an attractive choice for large scale quantum technology integration [5].

Superconducting silicon is achievable by incorporating boron above the solid limit solubility. Heavily boron-doped superconducting silicon has been demonstrated for the first time with the Gas Immersion Laser Doping technique (GILD) combining BCl_3 precursor gas chemisorption and UV-NLA at melt condition [6-8]. Then, the same research team succeeded in obtaining superconducting silicon by using ion implantation and UV-NLA in ultra-high vacuum atmosphere [9].

In this paper, we present the properties of superconducting heavily boron-doped poly-SOI fabricated by ion implantation and UV-NLA process in industrial conditions (atmospheric pressure, N_2 flow). This constitutes a step forward towards the large scale integration of superconducting silicon.

2. Experimental details

We started from a 300 mm wafer with 15 nm of Si (CZ, p-type, 5-15 Ω.cm, (001) orientation) on top of 20 nm of Buried OXide (BOX), itself on top of bulk (100) silicon (CZ, n-type). The wafer was first thickened to 33 nm in a reduced pressure chemical vapor deposition (CVD) tool. Then, a boron implantation at 3 keV with a total dose of 2.5 x 10^{16} cm^{-2} was performed. The post implantation SOI layer was partially

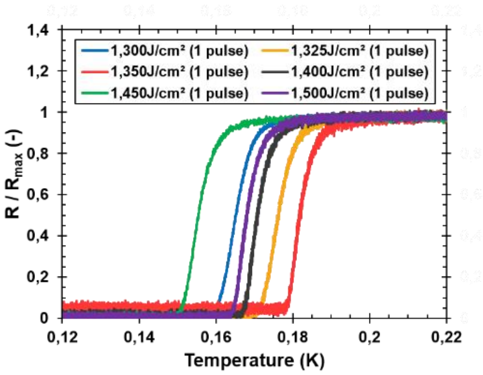

Fig. 1: Normalized resistance as a function of temperature of heavily boron-doped SOI layers annealed at ED between 1.3 and 1.5 J/cm² (1 pulse).

amorphized (15 nm upper region) with a 19 nm thick crystalline seed below (Fig. 2a). The last step consisted in a UV-NLA with an industrial SCREEN-LASSE (LT3100) tool (λ=308 nm, pulse duration=160 ns, 4 Hz repetition rate, 15 x 15 mm²) on a chuck stabilized at 200 °C under N_2 at atmospheric pressure. We explored different laser conditions: 1 pulse (0.4 to 1.5 J/cm², 0.025 J/cm² incremental steps) and 1, 3, 10 and 100 pulses (0.6 to 1.5 J/cm², 0.05 J/cm² incremental steps).

3. Results and discussions

Single pulse low temperature results

We studied resistance variations as a function of temperature for energy densities (ED) between 0.4 and 1.5 J/cm² for 1 pulse annealing (Fig. 1). We observed three different behaviors: resistive (ED<1.25 J/cm²), partially superconducting (1.275 J/cm²) and superconducting (ED≥1.3 J/cm²). From curves presented in Fig. 1, we extracted an average critical temperature of 169.3 ± 9.3 mK.

By combining 4-point probe (4PP), haze, transmission electron microscopy (TEM) (shown in Fig. 2), atom force microscopy (AFM) and time-resolved reflectivity (TRR) measurements (not shown), five regimes were identified (graph on Fig. 2d). Between 0.7 and 0.775 J/cm², the NLA thermal budget was not sufficient to reach the melt temperature of amorphous or crystalline silicon: sub-melt regime (1). For ED between 0.775 to 0.9 J/cm², fast and exclusive melt of the amorphous silicon occurred prior to fast solidification into

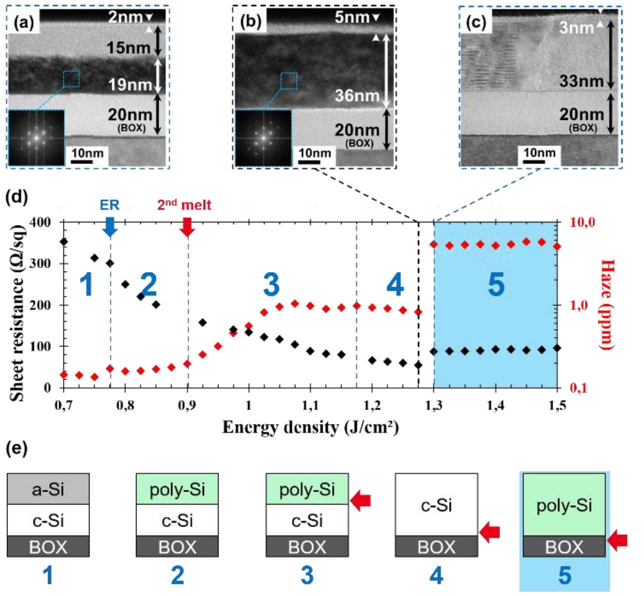

Fig. 2: Cross section TEM images of heavily boron-doped SOI layers after boron implantation (a) and after UV-NLA (1 pulse) at 1.275 J/cm² (b) and 1.3 J/cm² (c). Sheet resistance and haze measurements as a function of energy density for 1 pulse NLA (d). Schematics of SOI layer evolution as a function of ED (e).

poly-Si with the so-called explosive recrystallization (ER) [10] (2). From 0.9 J/cm², ER is directly followed by a second melt. As the melt depth increases with energy density, we observe three different results (red arrows in Fig. 2e). If the melt depth is inferior to the poly-Si thickness, the final system is poly-Si on top of c-Si (3) (possibly with different grain size than ER poly-Si). If the melt depth exceeds the poly-Si thickness while being less deeper than the SOI thickness, the resulting layer is monocrystalline silicon (4). For energy densities between 1.300 and 1.5 J/cm², the front melt reaches the c-Si/BOX interface, leaving no seed for recrystallization. Then, the final layer becomes entirely polycrystalline (5). TEM characterizations in bright field on samples annealed at 1.275 and 1.3 J/cm² (Fig 2b and 2c) confirmed the full-melt energy density threshold. Indeed, at 1.275 J/cm², the entire SOI layer was monocrystalline (diffraction figure in Fig 2b) while at 1.3 J/cm², the layer was polycrystalline/amorphous (Fig 2c).

Thanks to both low temperature results and room temperature characterizations (presented in Fig. 2), we identified full melt threshold as a clear process window to obtain superconducting SOI layers.

Low-temperature measurements under magnetic field

We performed low temperature measurements under variable magnetic fields from 0 to 0.05 T with 0.005 T increments for different NLA full-melt conditions. Curves presented in Fig. 3 give the critical field variation as a function of critical temperature. All curves are linear with comparable slopes (average of -0.39 ± 0.04 T/K) whatever the number of pulses and the ED. Comparing mean free path l (see eq. (1)) and coherence length ξ gives ξ~20 μm >> l~1 nm, placing our

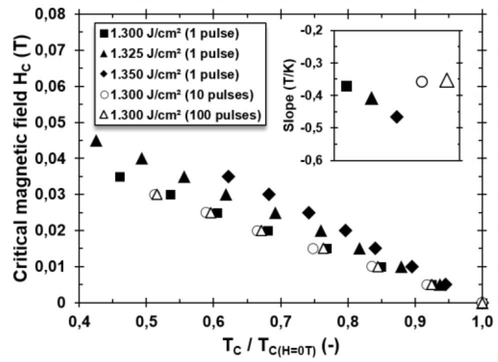

Fig. 3: Variations of the normalized critical temperature with applied magnetic field and slope (inset) measured on superconducting SOI layers fabricated by ion implantation and NLA.

system in the dirty limit (type II superconductor in the Ginzburg-Landau formalism).Thanks to eq. (2), we estimated the real coherence length (affected by strong impurity effect [10]) to be around 75 nm.

$$l = \frac{v_F}{\rho e^2}\left(\frac{m^*}{n}\right) \quad (1)$$

$$H_{c_2} = \frac{3\Phi_0}{2\pi^2 \xi l} \quad (2)$$

3. Conclusion

We demonstrated the first reproducible process to fabricate heavily boron-doped ultrathin superconductive poly-SOI layers by ion implantation and UV-NLA under N_2 flow at atmospheric pressure. Complete melt of the SOI layer was found to be a necessary condition to obtain superconductive samples. All critical temperatures were between 150 and 200 mK. Low temperature measurements under magnetic field revealed a type II superconductor behavior with a coherence length around 75 nm.

Acknowledgements

This work has been supported by the French ANR through Carnot funding. We are grateful to J.-M. Hartmann, D. Debarre and F. Chiodi for fruitful discussions and to SCREEN-LASSE company for its support in the maintenance and operation of the UV-NLA system.

References

[1] M. H. Devoret *et al.*, Science **339** (2013) 1169.
[2] K. Saeedi *et al.*, Science **342** (2013) 830.
[3] J. T. Muhonen *et al.*, Nature Nanotech. **9** (2014) 986.
[4] T. Brecht *et al.*, npj Quantum Information **2** (2016) 16002.
[5] Y. Shim *et al.*, Nat. Comm. **5** (2014) 4225.
[6] E. Bustarret *et al.*, Nature **444** (2006) 465.
[7] A. Grockwiak *et al.*, Phys. Rev. B **88** (2013) 064508.
[8] C. Marcenat *et al.*, Phys. Rev. B **81** (2010) 020501.
[9] A. Grockowiak *et al.*, Supercond. Sci. Tech. **26** (2013) 045009.
[10] L. Nikolova et al., J. Appl. Phys. 116 (2014) 093512.
[11] M. Kriener et al., Phys. Rev. B **78** (2008) 024517.